Dalton Transactions

PAPER

View Article Online
View Journal | View Issue

Cite this: *Dalton Trans.*, 2015, **44**, 12863

Tuning of exchange coupling by the Mn–O distance and phenoxido bridging angle: an experimental and theoretical study of the family of Mn(III) dimers with salen type ligands†

Piya Seth, Sanjib Giri and Ashutosh Ghosh*

Received 27th March 2015,
Accepted 29th May 2015

DOI: 10.1039/c5dt01224d

www.rsc.org/dalton

Three new Mn(III) complexes $[Mn_2L_2(ClO_4)_2]$ (**1**), $[Mn_2L_2(NCS)_2]$ (**2**) and $[Mn_2L_2N(CN)_2]ClO_4{\cdot}CH_3CN$ (**3**) have been synthesized from the Schiff base ligand H_2L (where H_2L = *N*,*N*′-bis(2-hydroxypropiophenone)-1,2-ethanediamine) and various anionic coligands *e.g.* perchlorate, thiocyanate and dicyanamide. X-ray crystal structure analysis reveals that **1** and **2** are dinuclear complexes, joined together by Mn···O (phenoxido) interactions. Whereas **3** consists of an alternating phenoxido and $\mu_{1,5}$ dicyanamido bridge, resulting in a 1D chain. In **1** and **2** ferromagnetic coupling exists between the Mn(III) centres within the dimer but **3** possesses antiferromagnetic interaction. This difference in magnetic exchange interactions has been rationalized on the basis of structural parameters like longer bridging Mn–O distance and Mn–O–Mn angle in these complexes with the help of DFT calculations.

Introduction

Exchange interactions between the metal centers in polynuclear manganese(III) complexes of Schiff base ligands have received wide attention in the field of molecular magnetism for investigations of magnetic properties and structural correlation of these complexes.[1] Some of these complexes have been extensively studied for their potential to act as single molecule magnets (SMMs)[2] or single-chain magnets (SCMs).[3] In addition, these complexes are unique systems for studying quantum spin tunnelling and quantum phase interference leading to their applications in molecular electronics.[4]

Binuclear phenoxido bridged manganese(III) compounds of salen-type Schiff bases are well established, and are of interest to chemists because of their significant roles in the field of molecular magnetism and also in biological systems *e.g.* metalloenzymes, redox and non-redox proteins,[5,6] and as catalysts in olefin epoxidation reactions.[7] The study of magnetic properties of these complexes reveals that some of them exhibit antiferromagnetic intra-dimer interaction whereas some other complexes undergo intra-dimer ferromagnetic exchange which affords an $S = 4$ ground spin state to show the characteristic SMM behaviour.[1b,2b,8] From the literature survey, it is found that the $Mn^{III}\cdots Mn^{III}$ magnetic interaction of these dimeric complexes is modulated by Mn–O (phenoxido) distances.[1b] For ferromagnetic complexes Mn–O distances are relatively long compared to those of the antiferromagnetic compounds.[1d] For most of the Mn(III) dimeric complexes ferromagnetic interaction can be explained as the result of the d_{z^2} and the d_π (d_{xy}, d_{yz}, and d_{xz}) orbital orthogonality.[1b,d] With an increase in the Mn–O distance ferromagnetic interaction in the dimeric core decreases *i.e.* J value decreases. However, for few complexes the exchange coupling constant (J) exhibits a reverse relationship with the Mn–O distance *i.e.* with an increase in Mn–O distance the J value increases. In order to explain this apparent anomaly it was predicted that another structural parameter, phenoxido bridging (Mn–O–Mn) angle, might be responsible for this.[1b,9,10] It was anticipated that the wider Mn–O–Mn angle might cause antiferromagnetic coupling to take place between the Mn(III) centres in phenoxido bridged dimers. But to explain the magnetic behaviour of all such types of complexes, the effect of the Mn–O–Mn angle has not been emphasized to date. It is to be mentioned here that the correlation of magnetic exchange coupling of these Mn(III) dimers with both the structural parameters *viz.* Mn–O distance, Mn–O–Mn angle remains unexplored so far.

With an aim to study the magneto-structural correlations for these phenoxido bridged Mn(III) dimers, we report the synthesis, crystal structure, and magnetic properties of three new Mn(III) Schiff-base complexes $[Mn_2L_2(ClO_4)_2]$ (**1**),

Department of Chemistry, University College of Science, University of Calcutta, 92, A.P.C. Road, Kolkata 700 009, India. E-mail: ghosh_59@yahoo.com

†Electronic supplementary information (ESI) available: Dimensions in a metal coordination sphere of **1–3**, field dependent magnetization and various DFT results in a tabular form. CCDC 1055252 (**1**), 1055253 (**2**) and 1055254 (**3**). For ESI and crystallographic data in CIF or other electronic format see DOI: 10.1039/c5dt01224d

$[Mn_2L_2(NCS)_2]$ (**2**) and $[Mn_2L_2N(CN)_2]ClO_4{\cdot}CH_3CN$ (**3**), where H_2L = *N*,*N*′-bis(2-hydroxypropiophenone)-1,2-ethanediamine. With ClO_4^- and NCS^- anions we obtain dinuclear complexes, joined together by weak Mn···O (phenoxido) interactions. In **3**, there is an alternating phenoxido and $\mu_{1,5}$ dicyanamido bridge to result in a 1D chain. In **1** and **2**, ferromagnetic coupling exists between the Mn(III) centres within the dimer whereas **3** possesses antiferromagnetic interaction through the phenoxido bridge. We incorporate theoretical calculations by changing the longer bridging Mn–O distances to get an understanding of the magneto-structural correlation. However, for our complexes, the correlation with these Mn–O distances does not agree well. To get an insight into the magneto-structural correlations, we have also performed theoretical calculations to find the dependence of *J* on Mn–O–Mn phenoxido bridging angle. Besides, we have calculated *J* values for previously reported complexes and included in our study to obtain extensive magneto-structural correlations.

Experimental section

Starting materials

2′-Hydroxypropiophenone, 1,2-ethanediamine, sodium dicyanamide, and ammonium thiocyanate were of AR grade and were used without further purification.

Caution! perchlorate salts are potentially explosive. Only small amounts should be used and handled with great care.

Synthesis of the Schiff-base ligand *N*,*N*′-bis(2-hydroxypropiophenone)-1,2- ethanediamine (H_2L)

The di-Schiff base ligand, H_2L, was synthesized in our laboratory by standard methods.[11] 2′-Hydroxypropiophenone (1.37 mL, 10 mmol) was mixed with 1,2-ethanediamine (0.31 mL, 5 mmol) in methanol (20 mL). The resulting mixture was refluxed for *ca.* 1 h and allowed to cool. The desired yellow crystalline solid ligand was filtered, washed with methanol, and dried in a vacuum desiccator that contained anhydrous $CaCl_2$.

Synthesis of $[Mn_2L_2(ClO_4)_2]$ (1) and $[Mn_2L_2(NCS)_2]$ (2)

A methanolic solution (10 mL) of the ligand H_2L (0.324 g, 1 mmol) was mixed with 2 mmol (0.28 mL) of triethylamine. To it a methanolic solution (5 mL) of $Mn(ClO_4)_2{\cdot}6H_2O$ (0.361 g, 1 mmol) was added drop wise with constant stirring. The resulting solution was stirred for half an hour. It was then filtered and the filtrate was placed in a beaker in covered conditions for slow evaporation of the solvent. After 2–3 days dark brown, X-ray quality single crystals were obtained on the wall of the beaker. The crystals were isolated, washed with methanol, and dried in a desiccator containing anhydrous $CaCl_2$.

For synthesis of **2** the same procedure has been followed along with the dropwise addition of a 1 : 10 H_2O–MeOH (v/v, 10 mL) mixture of 1 mmol (0.076 g) of NH_4SCN solution during stirring.

Complex **1**: Yield (78%): $C_{40}H_{44}N_4O_{12}Cl_2Mn_2$ (953.57): calcd C, 50.60; H, 4.25; N, 5.90; found C, 50.48; H, 4.22; N, 5.81. IR (KBr pellet, cm^{-1}) 1597 ν(C═N), 1086 $\nu(ClO_4)$.

Complex **2**: Yield (75%): $C_{42}H_{44}N_6O_4S_2Mn_2$ (870.83): calcd C, 57.93; H, 5.09; N, 9.65; found C, 57.80; H, 5.03; N, 9.52. IR (KBr pellet, cm^{-1}) 2058 ν(NCS), 1595 ν(C═N).

Synthesis of $[Mn_2L_2N(CN)_2]ClO_4{\cdot}CH_3CN$ (3)

In the case of **3** a 1 : 10 H_2O–MeOH (v/v, 10 mL) mixture of 1 mmol (0.090 g) of $NaN(CN)_2$ solution was added to the mixture containing H_2L, Et_3N and $Mn(ClO_4)_2{\cdot}6H_2O$ in methanol with constant stirring. The resulting solution was filtered and the filtrate was placed overnight in a beaker in covered conditions. A brown crystalline compound was separated on the next day which was redissolved in acetonitrile. Layering of this solution with Et_2O afforded well-formed X-ray quality single crystals.

Complex **3**: $C_{46}H_{50}N_9O_8ClMn_2$ (1002.28): calcd C, 74.04; H, 7.46; N, 8.64; found C, 73.88; H, 7.41; N, 8.52. (KBr pellet, cm^{-1}) 2375, 2346, 2162 $\nu(N(CN)_2)$, 1597 ν(C═N), 1098 $\nu(ClO_4)$.

Physical measurements

Elemental analyses (C, H, and N) were performed using a Perkin-Elmer 240C elemental analyzer. IR spectra in KBr (4000–500 cm^{-1}) were recorded using a Perkin-Elmer RXI FTIR spectrophotometer. Electronic spectra in acetonitrile (600–300 nm) were recorded in a Hitachi U-3501 spectrophotometer. Temperature-dependent molar susceptibility measurements of powdered samples of **1–3** were performed by a superconducting quantum interference device vibrating sample magnetometer (SQUID-VSM, Quantum Design) with an applied field of 500 Oe in the temperature range 2–300 K. The field dependent magnetic measurements (0–5 T) were carried out at 2 K for **1** and **2** and 1.8 K for **3**.

Crystal data collection and refinement

X-ray quality single crystals of complexes **1–3** were mounted on a Bruker-AXS SMART APEX II diffractometer equipped with a graphite monochromator and Mo-Kα (λ = 0.71073 Å) radiation. The crystals were positioned at 60 mm from the CCD. 360 frames were measured with a counting time of 10 s. The structures were solved by the Patterson method using SHELXS 97. Subsequent difference Fourier synthesis and least-square refinement revealed the positions of the remaining non-hydrogen atoms that were refined with independent anisotropic displacement parameters. Hydrogen atoms were placed in idealized positions and their displacement parameters were fixed to be 1.2 times larger than those of the attached non-hydrogen atom. Absorption corrections were carried out using the SADABS program.[12] All calculations were carried out using SHELXS 97,[13] SHELXL 97,[14] PLATON 99,[15] and ORTEP-32.[16] Data collection, structure refinement parameters and crystallographic data for the three complexes are given in Table 1.

Table 1 Crystal data and structure refinement of complexes **1–3**

	1	**2**	**3**
Formula	$C_{40}H_{44}N_4O_{12}Cl_2Mn_2$	$C_{42}H_{44}N_6O_4S_2Mn_2$	$C_{46}H_{50}N_9O_8ClMn_2$
Formula weight	953.57	870.85	1002.28
Space group	$P2_1/n$	$P2_1/n$	$P\bar{1}$
Crystal system	Monoclinic	Monoclinic	Triclinic
a/Å	8.475(1)	8.454(2)	12.408(5)
b/Å	19.475(3)	20.424(4)	12.628(5)
c/Å	12.112(2)	11.755(3)	17.325(7)
α/°			78.296(2)
β/°	93.477(2)	93.050(2)	78.296(5)
γ/°			63.082(2)
V/Å^3	1995.5(2)	2026.8(8)	2353.2(2)
Z	2	2	2
Calculated density D_{calc}/g cm^{-3}	1.587	1.427	1.414
Absorption coeff. (μ)/mm^{-1}	0.837	0.776	0.656
F(000)	984	904	1040
R(int)	0.039	0.042	0.053
θ range (°)	2.0, 25.0	2.0, 25.2	1.2, 25.4
Total reflections	13 719	9227	30 683
Unique reflections	3519	3531	8555
$I > 2\sigma(I)$	2691	2263	6460
R_1, wR_2	0.0362, 0.1284	0.0536, 0.1620	0.0445, 0.1514
Temp. (K)	293	293	293

Results and discussion

Syntheses, IR and UV-Vis spectra of the complexes

Complex **1** was obtained by the slow evaporation of a methanolic solution containing H_2L, Et_3N and $Mn(ClO_4)_2{\cdot}6H_2O$ in a 1 : 2 : 1 molar ratio. Complexes **2** and **3** were synthesized by a similar reaction of H_2L, Et_3N, $Mn(ClO_4)_2{\cdot}6H_2O$ and NH_4SCN (in **2**) or $NaN(CN)_2$ (in **3**) in a 1 : 2 : 1 : 1 molar ratio using H_2O–MeOH (1 : 10) as a solvent. In all three complexes the Mn(II) ion was oxidized by the aerial oxygen to Mn(III) under the reaction conditions and the donor atoms of the deprotonated ligand (H_2L) coordinate to form the equatorial plane of the Mn(III) site, as is usual for the salen-type Schiff base complexes. **1** and **2** are phenoxido bridged dimers containing the terminally coordinated anions *viz*. ClO_4^- and NCS^- respectively. Whereas **3** contains alternate phenoxido and $\mu_{1,5}$-$N(CN)_2$ bridges resulting in a one-dimensional chain (Scheme 1).

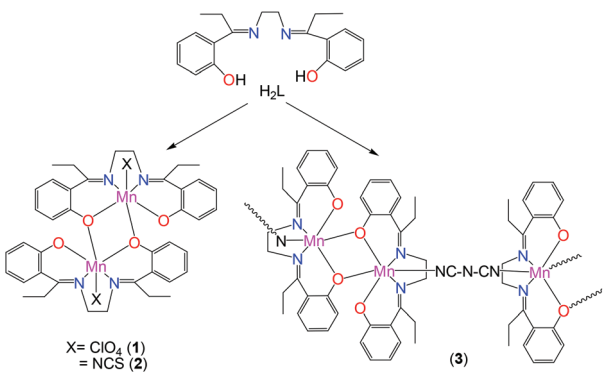

Scheme 1 Formation of complexes **1–3**.

Besides elemental analysis, all three complexes were characterized by IR spectra. The attributions of the IR spectra in the region 1595–1597 cm^{-1} can be assigned to the azomethine ν(C=N) group in **1–3**. Besides, IR spectra of **1** exhibit a strong absorption band at 1086 cm^{-1} due to the presence of a ClO_4^- anion and **2** has a sharp peak at 2058 cm^{-1} for an SCN^- anion. In **3**, the presence of a $N(CN)_2^-$ anion was confirmed by the appearance of three sharp and strong characteristic stretching frequencies at 2375, 2346 and 2162 cm^{-1} corresponding to ν_{as} + ν_s(C–N) combination modes, ν_{as}(C≡N) and ν_s(C≡N) vibrations[17] and a peak for a ClO_4^- anion was observed at 1098 cm^{-1}. UV-vis spectra of **1–3** in acetonitrile solvent show a broad band at 391 (for **1**), 398 (for **2**) and 385 nm (for **3**) corresponding to the ligand to metal charge transfer.[18]

Description of structures

Complexes **1** and **2** have similar structures, di-phenoxido bridged centrosymmetric dimers, are shown in Fig. 1 and 2 respectively. In both cases the Mn(III) centers are bonded to the four donor atoms (N(1), N(2), O(1), O(2)) of the deprotonated ligand in an equatorial plane with the axial sites consisting of an anion, perchlorate in **1** and thiocyanate in **2**, and an oxygen atom of a second ligand. In the equatorial plane Mn–O distances are 1.840(2)–1.894(2) Å in **1**, 1.851(3)–1.909(3) Å in **2** and Mn–N distances are 1.981(2)–1.985(2) Å in **1**, 1.983(4)–1.994(4) Å in **2**. The axial bond length Mn(1)–O(1)′ (where ′ = 1 − x, −y, 1 − z in **1**, −x, −y, 1 − z in **2**) is 2.337(2) and 2.418(3) Å in **1** and **2** respectively. The other axial position is occupied by a terminally coordinated perchlorate ion in **1** with Mn(1)–O(3) distance 2.300(3) Å and a thiocyanate ion in **2** with Mn(1)–N(3) distance 2.182(4) Å (Table ST1 in the ESI†).

The donor atoms in the equatorial plane show a r.m.s. deviation of 0.055 and 0.036 Å with the deviation of the metal

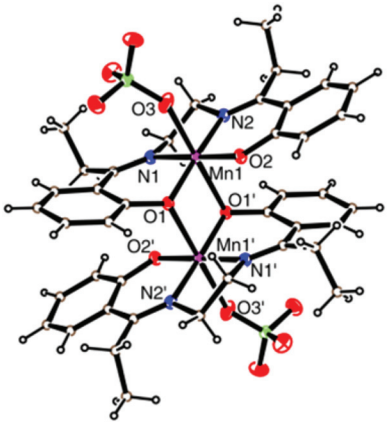

Fig. 1 The structure of centrosymmetric dimer **1** with ellipsoids at 30% probability.

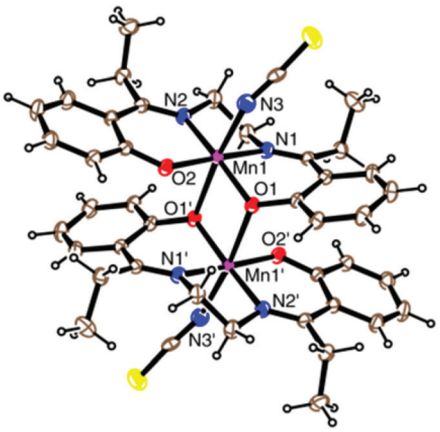

Fig. 2 The structure of centrosymmetric dimer **2** with ellipsoids at 30% probability.

0.074(1) and 0.148(1) Å from the plane to the direction of the anion in **1** and **2** respectively.

The crystal structure of **3** consists of a polymeric cation, perchlorate anion and solvent acetonitrile molecule (Fig. 3). The cationic part consists of two independent Mn atoms, each participating in a centrosymmetric dimer and connected to the adjacent one *via* $\mu_{1,5}$-dicyanamido bridges resulting in a 1-dimensional chain (Fig. 4). The coordination around Mn(1) is very much similar to that of **1** and **2**. It is bonded to the four donor atoms of the ligand (O(1), O(2), N(1), N(2)) in an equatorial plane with Mn–O distances 1.851(2) and 1.908(2) Å and Mn–N distances 1.990(3) and 2.001(2) Å. The axial sites are occupied by nitrogen (N5) of a bridging dicyanamide at a distance 2.251(3) Å and an oxygen atom (O2′) of a second ligand at a distance 2.373(2) Å (where ′ = 2 − *x*, 1 − *y*, −*z*). The other manganese center (Mn(2)) is coordinated to the donor atoms O(3), O(4), N(3), N(4) of the ligand with Mn–O distances 1.848(2) and 1.897(2) Å and Mn–N distances 1.989(2) and 1.996(3) Å. The axial positions are occupied by nitrogen (N(6)) of a bridging dicyanamide at a distance 2.210(4)Å and an oxygen atom

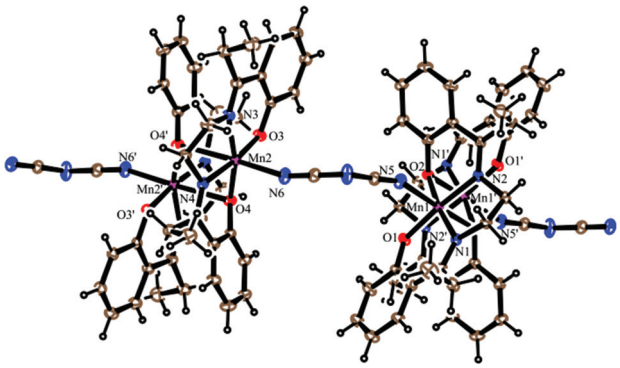

Fig. 3 The structure of **3** with ellipsoids at 20% probability. Perchlorate and acetonitrile molecules are omitted for clarity.

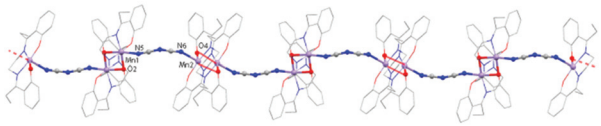

Fig. 4 Alternate phenoxido and $\mu_{1,5}$-dicyanamido bridges resulting in an 1-dimensional chain in **3**.

(O4″) of a second ligand at a distance 2.553(2) Å (where ″ = 1 − *x*, 1 − *y*, 1 − *z*) which is slightly greater than that of Mn(1)–O(2)′. The donor atoms in the equatorial plane show a r.m.s. deviation of 0.004 and 0.051 Å with the deviation of the metal 0.076(1) and 0.161(1) Å from the plane to the direction of the anion for Mn(1) and Mn(2) respectively.

Magnetic properties

Temperature-dependent magnetic susceptibility measurements on powdered samples of **1–3** were carried out in an applied field of 0.02 T in the temperature range 2–300 K. The data are shown in the $\chi_M T$ *versus* T plot in Fig. 5, where χ_M is the molar magnetic susceptibility and T is the absolute temperature. At room temperature, the values of $\chi_M T$ are 6.741, 6.271 and 6.203 cm^3 K mol^{-1} for **1**, **2** and **3** respectively, which are in agreement with the expected value of two non-interacting Mn(III) ions with $S = 2$ spin. On lowering temperature, $\chi_M T$ values for **1** show a slow increment to reach a maximum of 6.86 cm^3 K mol^{-1} at 17 K followed by a rapid lowering to reach a value of 3.57 cm^3 K mol^{-1} at 2 K. The increasing $\chi_M T$ value with lowering temperature signifies a characteristic feature of moderate ferromagnetic interactions between the intra-molecular Mn(III) ions and the sharp decrease of $\chi_M T$ value at low temperature represents a characteristic feature of inter-molecular antiferromagnetic interaction and/or an anisotropy factor (D) that arises from zero-field splitting. Complex **2** exhibits a continuous rise of $\chi_M T$ values with the lowering of temperature that reaches 7.61 cm^3 K mol^{-1} at 2 K. This behavior indicates that a dominant ferromagnetic coupling is operative between Mn(III) ions within the dimeric unit. In contrast, the $\chi_M T$ values measured for **3** remain nearly constant at ~6.1 cm^3 K

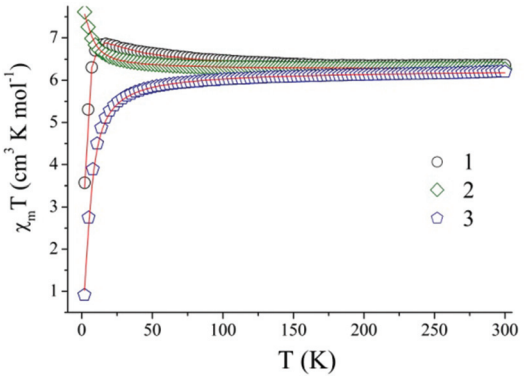

Fig. 5 Thermal dependence of $\chi_M T$ for complexes **1–3**. The points represent the experimental data and the associated solid lines are generated from the best fitted curve.

mol^{-1} down to 50 K and on further lowering, it shows a quick drop to reach a minimum value of 0.91 cm^3 K mol^{-1} at 2 K. This nature of the $\chi_M T$ plot suggests for a weak antiferromagnetic interaction in complex **3**.

Fig. S1 (ESI†) shows the variation of magnetization with fields at 2 K for **1** and **2** and 1.8 K for **3**. It is seen that the saturated molar magnetization value of **1** and **2** is ~6.75 BM at 5 T which is expected for Mn(III) dimers.[9] Due to intermolecular antiferromagnetic interactions and/or zero field splitting, the magnetic saturation curve of **1** is steeper at lower field (zero to ~1 T) than **2**. In contrast, the magnetization value of **3** is very much lower than that of **1** or **2**. It also shows a relatively slow increase of M values from zero to ~1 T; however, at higher field (1 T to 3 T) it increases more rapidly. This indication represents that initially (from 0 to 1 T) the spins are resisted from being ordered through the field direction because of the antiferromagnetic coupling.

The magnetic properties of these three complexes were analyzed by a theoretical model considering the interaction between two $S = 2$ spin centers. Due to the larger Mn–Mn distances through dicyanamide bridging we have ignored the associated small interactions through this bridge in complex **3**. To account for the low temperature behavior, we have considered molecular field approximation to include the intermolecular interaction (zJ'). As the anisotropy factor (D) is already included in the intermolecular interaction (zJ') part, it is not feasible to extract the D parameter separately from intermolecular (zJ') contributions. The total spin Hamiltonian taking into account the Zeeman perturbation for the dimer is given in the following equations:

$$H = -J\hat{S}_{Mn1}\hat{S}_{Mn2} + g_{Mn}\beta(\hat{S}_{Mn1} + \hat{S}_{Mn2})H,$$

$$\chi_M T = \frac{Ng^2\beta^2 xT}{kT - zJ'x}$$

$$x = \frac{60 + 2\exp\left(-\frac{9J}{kT}\right) + 10\exp\left(-\frac{7J}{kT}\right) + 28\exp\left(-\frac{4J}{kT}\right)}{9 + 3\exp\left(-\frac{9J}{kT}\right) + 5\exp\left(-\frac{7J}{kT}\right) + 7\exp\left(-\frac{4J}{kT}\right) + \exp\left(-\frac{10J}{kT}\right)}$$

where J represents the Mn–Mn exchange coupling parameter. S_{Mn} and g_{Mn} are spin and the local g-tensor associated with Mn(III) respectively. The best agreement between experimental and simulated curves was obtained with the following sets of parameters: $g = 2.04(5)$, $J = 1.95(2)$ cm^{-1}, $J' = -0.41(1)$ cm^{-1}, $R = 2 \times 10^{-5}$ for **1**, $g = 2.04(1)$, $J = 0.44(1)$ cm^{-1}, $J' = 0.051(1)$ cm^{-1}, $R = 2.4 \times 10^{-6}$ for **2** and $g = 2.03(6)$, $J = -1.07(1)$ cm^{-1}, $J' = 0$ cm^{-1}, $R = 2.5 \times 10^{-5}$ for **3**. Here, R represents the agreement factor defined as $R = \sum[(\chi_M T)_{exp} - (\chi_M T)_{calc}]^2/\sum(\chi_M T)_{exp}$. It is noteworthy that the data fitting for **1** with only anisotropy term (D) in spin Hamiltonian results in a relatively poor fitted curve and have considerable deviation at the low temperature regime. This signifies that both intra-dimer coupling and ZFS are dominant and that's why these components are not evaluated independently.[19]

Computational methodology

To calculate the theoretical coupling constant (J) of these complexes, we have used DFT calculations to compute two energy levels of high spin (E_{hs}) and broken symmetry (E_{bs}) states. Then, the J values have been derived from eqn (1) as proposed by Ruiz *et al.*[20] The hybrid B3LYP functional[21–23] and the TZVP[24] basis set have been used in all calculations as implemented in the ORCA package.[25] We have included zeroth-order regular approximation (ZORA) to describe scalar relativistic effects and tight SCF convergence criteria (Grid4) for all calculations.[26] To speed up the calculations, we have used RI approximation with auxiliary TZV/J coulomb fitting basis sets.[27] The energy calculations were carried out by considering all the experimental X-ray structures without further geometrical optimization. In order to perform longer bridging Mn–O distance & Mn–O–Mn angle dependent DFT calculations, we have varied Mn–O distances and Mn–O–Mn angles independently, maintaining the rest of the structure unaltered.[28] Variation of bond lengths was performed by changing the distance of two monomeric MnO_2N_2 units along the Mn–O bond and variation of bond angles was made by moving one of Mn–O_2N_2 units along the Mn–O bond (for details see the ESI†).

$$J = \frac{E_{bs} - E_{hs}}{2S_1S_2 + S_1} \quad (1)$$

where $S_1 \geq S_2$.

Magneto-structural correlations

To achieve magneto-structural correlation, we have performed DFT calculations with the broken-symmetry approach which gives the following value of $J = 0.347$, 0.093, and −0.869 cm^{-1} for **1**, **2** and **3** respectively, which fairly agrees with the experimentally obtained values as listed in Table 2. Although, the theoretically calculated J values are lower than the experimental ones for all three complexes, it still matches with sign and order. Due to the presence of two different types of Mn_2 cores with Mn–O distances (2.373 Å and 2.553 Å) in complex **3**, the calculation ended with two different J values of −1.650 and

Table 2 Magnetic and structural parameters of complexes **1–3**

Complex	Mn–O distance (Å)	Mn–O–Mn angle (°)	Coupling constant (J) Ruiz (cm^{-1})	Coupling constant (J) Experimental (cm^{-1})
1	2.337(2)	99.20(7)	0.347	1.95(2)
2	2.418(3)	99.98(1)	0.093	0.44(1)
3_1[b]	2.373(2)	101.50(9)	−1.650	−1.07[a](1)
3_2	2.553(2)	99.96(8)	−0.0879	

[a] Using the dimer model. [b] Complex **3** crystallized with two different dimeric units, for specifying we have denoted it **3_1** and **3_2**.

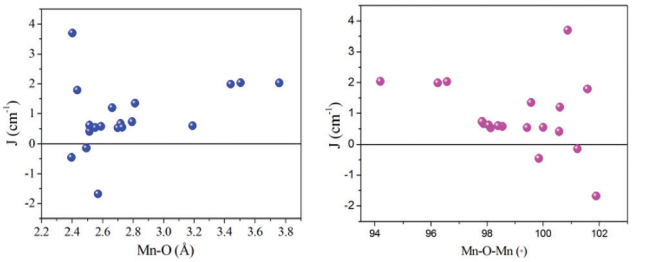

Fig. 6 Variation of J values (experimental) in phenoxido bridged Mn(III) dimers of salen type Schiff base ligands with Mn–O distance (left) and Mn–O–Mn angle (right).

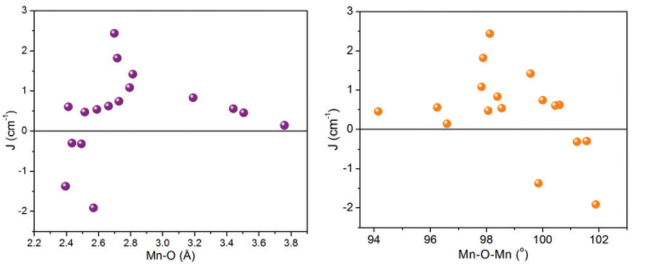

Fig. 7 Variation of J values (theoretical) in phenoxido bridged Mn(III) dimers of salen type Schiff base ligands with Mn–O distance (left) and Mn–O–Mn angle (right).

−0.0879 cm^{-1} and their scalar mean value is −0.869 cm^{-1} which is still lower than the experimentally obtained value of −1.07 cm^{-1}.

In the case of **1** and **2** the two Mn(III) centers are connected *via* a weak phenoxido oxygen from the second ligand and in **3** these phenoxido bridged dimers are connected *via* $\mu_{1,5}$-dicyanamido bridges. From these complexes and some previously reported similar complexes[1b,10,19,29] it is clear that the nature and strength of the magnetic exchange interaction are dependent on Mn–O distance. It has been already established that the unequal bond lengths at two apical positions observed for phenoxido bridged Mn(III) complexes is due to Jahn–Teller distortion. Now for octahedron geometry around the Mn(III) centre ferromagnetic interaction between the metal ions is mainly due to the result of orthogonality of the d_{z^2} and d_π orbitals (d_{xy}, d_{yz}, and d_{xz} orbitals).[1b,d,29] If the Mn–O distance is relatively long than a critical value, ~2.4 Å, the effective overlap of magnetic orbitals is less and ferromagnetic interaction occurs due to spin localization, however, for a shorter distance the overlap of magnetic orbitals is greater which prefers delocalization of spins; as a result, antiferromagnetic coupling is obtained.[1b] Hence, for the occurrence of ferromagnetic exchange coupling between the two Mn(III) centers the Mn–O distance should be relatively long than for antiferromagnetic coupling. This is the case with most of the previously reported phenoxido bridged Mn(III) complexes. Among our complexes, **1** has Mn–O distance 2.337 Å and J value 1.95 cm^{-1}. In **2**, the Mn–O distance is higher (2.418 Å) than **1** and hence ferromagnetic interaction decreases (J = 0.44 cm^{-1}) as is also evident from previously reported complexes. In the case of **3** the Mn–O distance is 2.373 Å, which is in between **1** and **2**, but it possesses antiferromagnetic interaction (J = −1.07 cm^{-1}). This signifies that the correlation of J values with Mn–O distance is conflicting for these complexes. From the structural parameters (Table 2), it can be noted that **3** has a larger Mn–O–Mn angle than the other two complexes. Therefore, it can be said that the Mn–O–Mn angle should have some influence on magnetic exchange coupling and we have checked it by theoretical studies.

To corroborate the experimental dependence of the J value on longer bridging Mn–O distance and Mn–O–Mn angle for the reported complexes we have performed DFT calculations on these systems to obtain the theoretical J values. From the comparison of experimental and theoretical results (Fig. 6 & 7), it is clear that the magnitude of J (experimental) differs from the J (theoretical), but the nature of exchange coupling (ferro- or antiferromagnetic), *i.e.* the sign of J matches for all the cases except for two (CIF COXQEM and XITQEW).[1d,9] Both the theoretical and experimental results confirm that antiferromagnetic interaction between the two Mn(III) centers would occur at Mn–O distance <2.4 Å, and above this distance ferromagnetic interaction is likely to take place (Table 3).

As mentioned earlier, some complexes, including our systems show deviations from the magneto-structural correlation based on only the Mn–O distance. To understand this inconsistency, we have performed DFT calculations by varying the Mn–O distance and the Mn–O–Mn angle separately, keeping the rest of the structural parameters unaltered (for details see the ESI†).

The results show that there is a strong dependence of the exchange coupling constant with the Mn–O distance for both **2** and **3** as shown in Fig. 8 (data given in Table ST2 and 3 in the ESI†). It is seen that with the increase in the Mn–O distance (from ~2.25 Å), at first the magnitude of J decreases and reaches a minimum value at ~2.4 Å. Then it starts to increase through a broader range and approaches a maximum at ~3.1 Å; thereafter the values decrease and tend to zero at longer Mn–O distances. The nature of the curve in both cases is similar but in the case of **2** the J value is positive throughout

Table 3 DFT calculations for previously reported complexes

CCDC codes	Mn–O distance (Å)	Mn–O–Mn angle (°)	Coupling constant (J) Ruiz (cm^{-1})	Coupling constant (J) Experimental (cm^{-1})
IDEGUU	2.813	99.57	1.4202	2.7
IDEHAB	3.19	98.39	0.8316	1.2
IDEHEF	2.793	97.82	1.0859	1.46
IDEHIJ	2.727	100.0	0.7428	1.1
IDEHOP	2.395	99.85	−1.3711	−0.9
KUCQIJ01	2.699	98.12	2.4314	1.06
MURXED	2.717	97.88	1.8189	1.34
MURXIH	2.569	101.89	−1.9147	−3.36
XITQEW	2.434	101.57	−0.2932	3.58
XITQIA	2.662	100.60	0.6189	2.4
XITQOG	3.441	96.24	0.5537	3.98
XITQUM	3.758	96.59	0.1428	4.06
XITREX	3.506	94.15	0.4516	4.08
COXQEM	2.513	100.58	−0.1401	0.84
COXQIQ	2.589	98.54	0.5369	1.16
COXQOW	2.493	101.23	−0.3110	−0.276
COXQIQ01	2.514	98.06	0.4713	1.24
EYEJOH	2.411	100.45	0.6038	3.7

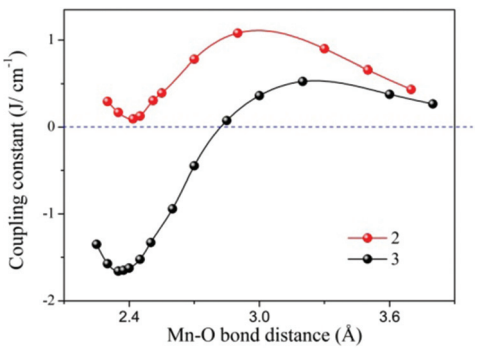

Fig. 8 Dependence of the calculated exchange coupling constant on Mn–O distance in **2** and **3_1**.

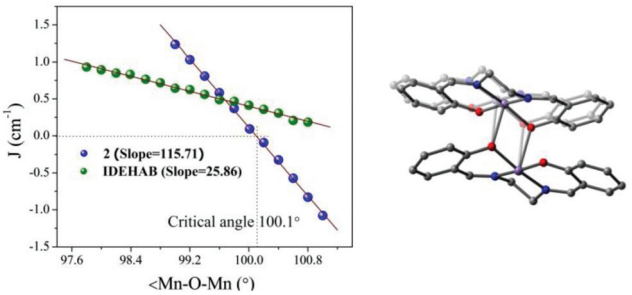

Fig. 9 Dependence of the calculated exchange coupling constant on Mn–O–Mn angle in **2** and a previously reported complex (CIF IDEHAB). (left) A view of complex **2** showing structural changes before and after modification of Mn–O–Mn angle, keeping Mn–O distance unaltered. (right) The modified structure is shown by faded fragments. Here, hydrogens, ethyl groups and coordinated thiocyanate anions are omitted for clarity.

the Mn–O distance range. However, in **3**, J value is initially negative up to the Mn–O distance ~2.7 Å and thereafter approaches positive values. Hence, we have checked the influence of the phenoxido bridging angle on J values by keeping the Mn–O distance unaltered (data given in Table ST4 in the ESI†). We have selected complex **2** from our system to perform this study. From Fig. 9, it is clear that there is a linear dependence of the J value on the Mn–O–Mn angle and with increase in the angle, the J value decreases. In complex **2**, the J value ranges from −1.07 to 1.25 cm^{-1} for variation of the Mn–O–Mn angle from 99.0 to 101.0°. There occurs a crossover from ferro- to antiferromagnetic behaviour during the course of variation in the Mn–O–Mn angle. From this calculation we have found theoretically that the crossover angle is 100.1° for **2**. To detect the dependence of the J value on the phenoxido bridging angle for complexes with a higher Mn–O distance (>3.0 Å) we have also performed a similar study with a previously reported complex (CIF IDEHAB)[1b] where the Mn–O distance is 3.19 Å. In this case, with the variation of the Mn–O–Mn angle in the range 97.7–100.8°, J value changes only slightly (0.2–0.94 cm^{-1}) and there is no change of sign of J. The slope of the curve for **2** is 4.47 times larger than that of IDEHAB. From this result, it is clear that for complexes with a higher Mn–O distance (>3.0 Å), the phenoxido bridging angle has only a trivial influence on magnetic exchange coupling.

From the combined study, we can conclude that the coupling is expected to be ferromagnetic in the complexes having a lower Mn–O–Mn angle (~99°) irrespective of the Mn–O bond distances. The complexes with shorter Mn–O distance (2.3–2.5 Å) have stronger influence of the Mn–O–Mn angle on J values. For these complexes the magnetic interaction becomes antiferromagnetic at larger Mn–O–Mn angles and at lower angles ferromagnetic interaction prevails. On the other hand, for complexes with higher Mn–O distance (>3.0 Å) the nature of magnetic exchange does not significantly change with the Mn–O–Mn angle and complexes remain ferromagnetic upto a much wider angle.

In summary, both the structural parameters *viz.* Mn–O distance and Mn–O–Mn angle have significant influences on magnetic coupling (J). If we choose to correlate for complexes with very close Mn–O distances, then the Mn–O–Mn angle is the dominating structural parameter to make an effective change of J values. In our complexes, the Mn–O distance varies from 2.337 to 2.418 Å, which is too small to make an effective change of J values. Therefore, it is obvious that the Mn–O–Mn angle has more control on modulating J values for our cases and also in the complexes reported by Bhargavi and Mandal *et al.*[9,10]

Conclusions

Three new phenoxido bridged Mn(III) complexes derived from a salen type Schiff base ligand have been synthesized and characterized in order to study the magneto-structural corre-

lations. Complexes **1** and **2** are di-phenoxido bridged centrosymmetric dimers whereas **3** consists of alternating phenoxido and $\mu_{1,5}$ dicyanamido bridges, resulting in a 1D chain. We have determined the *J* values of these complexes experimentally and corroborated it by means of DFT calculations. From the experimental and theoretical results of the present complexes and previously reported complexes, we show that *J* value does not solely depend on longer Mn–O distance but also on Mn–O–Mn angle. From DFT studies it has been verified that there is a linear dependence of *J* value on the Mn–O–Mn angle and with an increase in the angle *J* value decreases. In the complexes having a relatively small Mn–O distance, the Mn–O–Mn angle is the dominating structural parameter for interpreting the magnetic interaction especially when the variation of Mn–O distance is restricted within a short range as in the present complexes.

Acknowledgements

We thank the DST-FIST of India funded Single Crystal Diffractometer Facility at the Department of Chemistry, University of Calcutta, Kolkata, India. We also thank CRNN, University of Calcutta, Kolkata, India for magnetic measurement. The authors thank the Department of Science and Technology (DST), New Delhi, India, for financial support (SR/S1/IC/0034/2012). P.S. and S.G are grateful to the UGC, Government of India for a research fellowship (UGC/52/Jr. Fellow (Enhancement) and Dr D. S. Kothari fellowship (F.4-2/2006(BSR)/CH/13-14/0069) respectively.

References

1 (*a*) R. Karmakar, C. R. Choudhury, G. Bravic, J.-P. Sutter and S. Mitra, *Polyhedron*, 2004, **23**, 949–954; (*b*) Z. Lu, M. Yuan, F. Pan, S. Gao, D. Zhang and D. Zhu, *Inorg. Chem.*, 2006, **45**, 3538–3548; (*c*) H. Li, Z. J. Zhong, C. Duan, X. You, T. C. W. Mac and B. Wu, *J. Coord. Chem.*, 1997, **41**, 183; (*d*) H. Miyasaka, R. Clérac, T. Ishii, H.-C. Chang, S. Kitagawa and M. Yamashita, *J. Chem. Soc., Dalton Trans.*, 2002, 1528–1534.

2 (*a*) H. Hiraga, H. Miyasaka, R. Clerac, M. Fourmigue and M. Yamashita, *Inorg. Chem.*, 2009, **48**, 2887–2898; (*b*) P.-H. Lin, S. Gorelsky, D. Savard, T. J. Burchell, W. Wernsdorfer, R. Clérac and M. Murugesu, *Dalton Trans.*, 2010, **39**, 7650–7658; (*c*) S. Naiya, S. Biswas, M. G. B. Drew, C. J. Gómez-García and A. Ghosh, *Inorg. Chem.*, 2012, **51**, 5332–5341.

3 (*a*) P. Kar, R. Biswas, M. G. B. Drew, Y. Ida, T. Ishida and A. Ghosh, *Dalton Trans.*, 2011, **40**, 3295–3304; (*b*) C.-M. Liu, D.-Q. Zhang and D.-B. Zhu, *Inorg. Chem.*, 2009, **48**, 4980–4987.

4 (*a*) W. Wernsdorfer and R. Sessoli, *Science*, 1999, **284**, 133; (*b*) M. N. *Leuenberge*r and D. Loss, *Nature*, 2001, **410**, 789.

5 J. J. R. Frausto da Silva and R. J. P. Williams, *The Biological Chemistry of the Elements*, Clarendon Press, Oxford, 1991, ch. 14, p. 370.

6 *Manganese Redox Enzymes*, ed. V. L. Pecoraro, VCH, New York, 1992.

7 H.-L. Shyu, H.-H. Wei and Y. Wang, *Inorg. Chim. Acta*, 1999, **290**, 8–13.

8 H. Miyasaka, R. Clérac, W. Wernsdorfer, L. Lecren, C. Bonhomme, K. Sugiura and M. Yamashita, *Angew. Chem., Int. Ed.*, 2004, **43**, 2801–2805.

9 G. Bhargavi, M. V. Rajasekharan, J.-P. Costes and J.-P. Tuchagues, *Polyhedron*, 2009, **28**, 1253–1260.

10 S. Mandal, A. K. Rout, M. Fleck, G. Pilet, J. Ribas and D. Bandyopadhyay, *Inorg. Chim. Acta*, 2010, **363**, 2250–2258.

11 J. Reglinski, S. Morris and D. E. Stevenson, *Polyhedron*, 2002, **21**, 2167–2174.

12 SAINT, *version 6.02, SADABS, version 2.03*, Bruker AXS, Inc., Madison, WI, 2002.

13 G. M. Sheldrick, *SHELXS-97, Program for solution of crystal structures*, University of Göttingen, Germany, 1997.

14 G. M. Sheldrick, *SHELXL-97, Program for refinement of crystal structures*, University of Göttingen, Germany, 1997.

15 A. L. Spek, *Acta Crystallogr., Sect. A: Fundam. Crystallogr.*, 1990, **46**, C34.

16 L. J. Farrugia, *J. Appl. Crystallogr.*, 1997, **30**, 565.

17 (*a*) J. Carranza, C. Brennan, J. Sletten, F. Lloret and M. Julve, *J. Chem. Soc., Dalton Trans.*, 2002, 3164–3170; (*b*) L. K. Das and A. Ghosh, *CrystEngComm*, 2013, **15**, 9444–9456; (*c*) S. Ghosh, S. Mukherjee, P. Seth, P. S. Mukherjee and A. Ghosh, *Dalton Trans.*, 2013, **42**, 13554–13564.

18 P. Kar, P. M. Guha, M. G. B. Drew, T. Ishida and A. Ghosh, *Eur. J. Inorg. Chem.*, 2011, 2075–2085.

19 P. Mukherjee, M. G. B. Drew, V. Tangoulis, M. Estrader, C. Diaz and A. Ghosh, *Polyhedron*, 2009, **28**, 2989–2996.

20 E. Ruiz, A. Rodriguez-Fortea, J. Cano, S. Alvarez and P. Alemany, *J. Comput. Chem.*, 2003, **24**, 982–989.

21 A. D. Becke, *J. Chem. Phys.*, 1993, **98**, 5648–5652.

22 C. T. Lee, W. T. Yang and R. G. Parr, *Phys. Rev. B: Condens. Matter*, 1988, **37**, 785–789.

23 A. D. Becke, *Phys. Rev. A*, 1988, **38**, 3098–3100.

24 A. Schäfer, C. Huber and R. Ahlrichs, *J. Chem. Phys.*, 1994, **100**, 5829.

25 F. Neese, *ORCA, An ab initio, Density Functional and Semi-empirical Program Package, Version 3.0.2*, Universität Bonn, Bonn, Germany, 2014.

26 S. Giri, S. Biswas, M. G. B. Drew, A. Ghosh and S. K. Saha, *Inorg. Chim. Acta*, 2011, **368**, 152–156.

27 F. Weigend, *Phys. Chem. Chem. Phys.*, 2006, **8**, 1057.

28 R. Biswas, S. Giri, S. K. Saha and A. Ghosh, *Eur. J. Inorg. Chem.*, 2012, **17**, 2916–2927.

29 S. Mandal, G. Rosair, J. Ribas and D. Bandyopadhyay, *Inorg. Chim. Acta*, 2009, **362**, 2200–2204.

